ZINC OXIDE MEDIATED SOLAR PHOTOCATALYSIS

Abstract

Zinc oxide photo catalyst samples were synthesized by co-precipitation**,** solid state reaction and mechano chemical method. The photo catalysts thus prepared were characterized by various techniques such as powder XRD, SEM, EDX, XPS, TG-DTA, FT-IR, PL and UV-visible spectrophotometer. The solar photo catalytic activity of these semiconductors was examined by means of degradation of hazardous and endocrine disrupting chemicals such as Phenol, Resorcinol, and Bisphenol A in batch photo reactor. The effect of various parameters such as calcination temperature, amount of photo catalyst, concentration of substrate, pH of the suspension and sunlight irradiation time were investigated for maximum photo catalytic degradation (PCD) of these organic compounds. The extent of PCD was primarily determined in terms of decrease in absorbance while complete mineralization of substrate was confirmed by chemical oxygen demand (COD) method. The XRD data of pure ZnO matches to that of JCPDS card number J-36-1451 indexed for hexagonal wrutzite structure. Calcination temperature was found to affect the crystallite size and morphology of ZnO. The PCD of phenol, resorcinol and Bisphenol A (substrates) over ZnO was found to be more effective under solar light in comparison to artificial UV and visible light irradiation. Lower calcination temperature of photo catalyst (400 to 500^{o}C) favors PCD efficiency because of suitable morphology and optimum defect sites as a result of fast crystallite growth rate (E_1 = 1.88 kJ/mol). ZnO synthesized by mecha nochemical method shows better PCD efficiency in sunlight. The detailed mechanism of PCD of phenol**,** resorcinol and bisphenol A were proposed with the identification of intermediates.

Keywords: Photocatalysis, Zinc oxide, Sunlight, Degradation, Mechanochemical

Authors

Ashokrao B. Patil
Department of Chemistry
K. T. S. P. Mandal's
K. M. C. College,
Khopoli–Raigad Maharashtra.
abpatilchem23@gmail.com

Satish K. Pardeshi
Department of Chemistry
Savitribai Phule Pune University
(formerly University of Pune)
Ganeshkhind, Pune, India

I. INTRODUCTION

TiO_2 is the most often employed semiconductor among various photocatalysts. However, TiO_2 is only excited by ultraviolet light **[1, 2].** Use of UV light is not very practical or cost-effective. Researchers have now paid increasing attention to zinc oxide. Under solar radiation, zinc oxide is a well-known semiconductor whose photocatalytic process has been shown to be similar to that of TiO_2 **[3].** According to some reports, zinc oxide is more effective than titanium dioxide in some processes, such as the advanced oxidation of pulp mill bleaching waste water **[4].** The main benefit of ZnO is that it absorbs more of the solar spectrum than TiO_2 does **[5].** Because of this, ZnO is the best photocatalyst for the photocatalytic oxidation of organic molecules when sunshine is present. Photocatalysis using sunlight will be more cost-effective and preferred in nations with abundant sunlight since solar light contains roughly 43% visible and 4% ultra violet light, which is free and endless **[6].** When ZnO is irradiated with sunlight, the first step is generation of an electron-hole (e^-/h^+) pair results in the formation of hydroxyl radical ($^{\bullet}OH$), superoxide radical anions ($O_2^{\bullet-}$), and hydroperoxyl radical ($^{\bullet}OOH$). It is well known that hydroxyl radicals are potent and non-selective oxidising agents. (E^0 = +3.06 V), which are responsible for partial or complete mineralization of several organic pollutants **[7].** Additionally, the strong oxidative potential of the holes (h_{vb}^+) in the photocatalyst also allows the direct oxidation of organic pollutants to reactive intermediates. Very reactive hydroxyl radicals can also be created by the oxidation of holes or the decomposition of water or by the reaction of the hole with OH^-. The degradation efficiency depends on the concentration of oxygen and the extent of the recombination of electron-hole (e^-/h^+) prevention. The adsorbed substrate molecules can absorb the electron in the conduction band, resulting in the production of radical anion and the deterioration of the organic material **[8].** Numerous efforts have been made to stop the recombination of e/h+ and so increase the visible light photocatalytic activity of ZnO. Rongliang et al **[9]** reported visible light photocatalytic activity of polymer modified ZnO. Sobana and Swaminathan explored the combined effect of ZnO and activated carbon for solar-assisted photocatalytic degradation **[10].** The influence of production method of ZnO on its photocatalytic activity towards the photooxidation of 10 ppm phenol was investigated by Parida and Parija. **[11.** The manner of preparation and calcination temperature affect the morphology and crystallinity. Keeping this in mind, pure ZnO of various morphologies and crystallite sizes was produced using several techniques. Particle size and shape, surface area, and crystallinity all affect photocatalytic activity **[12].** ZnO of different morphologies were synthesized by Fang et al. **[13]** and Seow et al. **[14].**

This Chapter demonstrates the characterization and solar photocatalytic activity of zinc oxide synthesized by mechanochemical, solid state reaction and co-precipitation methods. As test reaction, the photocatalytic degradation of phenol, resorcinol and bisphenol A were used. In addition to effect of morphology and crystallite growth rate, other parameters such as photocatalyst amount, concentration of substrate, pH etc. on PCD efficiency is also studied.

II. SYNTHESIS OF PURE ZINC OXIDE

Photocatalytic effects of semiconductors have been of much interest from the viewpoint of solar energy utilization. In the present research, we have attempted to study systematically the effect of preparation method on the photocatalytic activity of ZnO towards the photooxidation of phenolic compounds under solar radiation. By using simple processes

like co-precipitation, solid state reactions and ecologically friendly and solution free mechanochemical technique, pure zinc oxide of various morphologies was produced.

1. **Co- precipitation method:** The zinc oxide was synthesized by co-precipitation method. Compared with other methods, the co-precipitation method makes the materials react uniformly at molecular level and has the advantages of lower polycrystalline-synthesis temperature and shorter sintering time. To get ZnO of different morphology, the precipitation agents as well as reaction conditions were varied as follows:

2. **Using zinc nitrate and sodium hydroxide:** In typical synthesis, 14.87g (0.05mol) of zinc nitrate (Zn $(NO_3)_2$. $6H_2O$) and 4.00g (0.1mol) of NaOH was dissolved separately in double distilled water and diluted to100 ml. Then the NaOH solution taken in gravimetric beaker was heated to 70^oC. Under constant magnetic stirring, zinc nitrate solution was then added slowly and dropwise to above alkali solution. The reaction mixture was then magnetically stirred for 2h at 70^oC. After 2h the white precipitate was collected and washed several times with double distilled water and absolute ethanol. The precipitate was then dried in open air. Finally, zinc oxide was obtained by calcination of dry precipitate in air atmosphere at 400^oC. This sample is named as **P1-Z4.**

3. **Using zinc acetate and sodium bicarbonate:** 10.975 g (0.05mol) of Zn $(CH_3COO)_2.2H_2O$ and 8.4g (0.1mol) of $NaHCO_3$ was dissolved separately in double distilled water and diluted to100 ml. Then $NaHCO_3$ solution was slowly added to the Zn $(CH_3COO)_2$ solution with continuous stirring till the pH of the solution became 7.0. The reaction mixture was then magnetically stirred for 1h. The precipitate was filtered, washed several times with distilled water, dried in open air and calcined in air atmosphere at 400^oC. This sample is named as **P2-Z4.**

4. **Solid state reaction method:** Matter is carried towards (or away from) an interface that separates the reactants and the result during a diffusion-controlled solid-state process. The reaction that occurs here, causing the contact to move and the development of a new phase. The progress of the reaction is strongly determined by the morphology of the interface**.**

   In a typical synthesis, 10.975 g (0.05 mol) of Zn $(CH_3COO)_2 \cdot 2H_2O$ was taken in agate mortar and hand ground for 5 min. Then 5 ml (0.035 mol) of Triethanol amine (TEA) was added to the Zn $(CH_3COO)_2 \cdot 2H_2O$ powder. The mixture was ground for next 5 min, and then it was stood for 2 h. The mixture that was still a solid power then mixed with 4.0g (0.1mol) of NaOH powder and further ground for 30 min. The product was washed several times in an ultrasonic bath with double distilled water and absolute ethanol to remove any by-product and TEA. Finally, the solid was dried and calcined in air atmosphere at 400^oC to obtain zinc oxide. This sample is named as **S-Z4.**

5. **Mechanochemical Method:** A mechanochemical process uses mechanical means to influence a chemical reaction. These techniques include several distinct grinding and milling techniques, including ball milling, colloidal milling, jet milling, and hand grinding. The particles of the reactants undergo a variety of modifications during milling or grinding, including deformation, friction, fracture, amorphization, quenching, and so forth. Later, at the reactant-reactant contacts, new product phase(s) is (are) produced. The product phase develops further and the chemical reaction is realised with the help of the

diffusion of atoms from the reactant phases, which form a barrier layer blocking further reaction. The key benefits are the ease of the synthetic process, effective mixing that results in a breakage and recombination of chemical bonds, and a reduction in energy and material costs. It has been extensively used in the manufacturing of ceramics, ferrites, ferroelectrics, mineral fertilisers, oxides, and building materials, as well as the activation of catalysts.

Zinc oxide crystallite was also prepared by solution free mechanochemical method. In a typical synthesis, 21.95g (0.1 mol) of zinc acetate and 15g (0.12 mol) of oxalic acid were mixed by grinding in an agate mortar for 30 minute at room temperature, forming the zinc oxalate dihydrate ($ZnC_2O_4 \cdot 2H_2O$). Zinc oxide crystallite was then prepared by thermal decomposition of the obtained zinc oxalate in air atmosphere at 400^{o}C. This sample is named as **M-Z4.** Photocatalytic activity depends upon calcination temperature because it affects surface morphology and crystallite size of zinc oxide. Therefore, zinc oxalate was calcined in air atmosphere from 500^{o}C to 800^{o}C, to obtain zinc oxide (**M-Z5, M-Z6, M-Z7 and M-Z8)** of different morphology and crystallite size.

III. CHARACTERIZATION OF ZINC OXIDE

Zinc oxide samples are then characterized by various techniques as discussed in following sections.

1. **TG-DTG analysis of zinc oxalate:** The TG-DTG curves of zinc oxalate dihydrate synthesized by mechanochemical method are shown in **Figure 1**. The TG curve shows two major weight loss processes from 30^{o}C to 390^{o}C. The first weight loss up to 120^{o}C (26.3%) was found to be greater than the theoretical weight loss (19.03%) expected for elimination of two molecules of water of crystallization. The difference in weight loss is attributed to the release of acetic acid byproduct as illustrated in **Scheme Ia, Chapter II**.

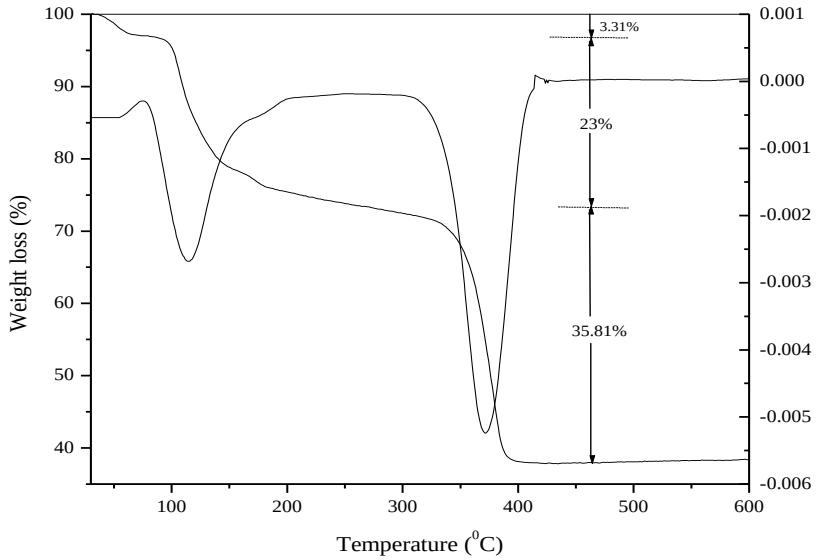

Figure 1: The TG-DTG analysis of zinc oxalate dihydrate

The 35.8% weight loss during second step of thermogram from 340 to 390^{o}C was found to match with calculated value of 36%; for oxalate group. There are two DTG peaks corresponding to weight loss processes indicated by TG curve. No further weight loss was observed from 400 to 800^{o}C, which suggests the formation of ZnO at 400^{o}C.

2. **FT-IR analysis: Figure 2** shows the FT-IR spectra of ZnO synthesized by mechanochemical method and samples calcined from 100^{o}C to 400^{o}C. FT-IR spectra of these samples show changes during the thermal decomposition process of zinc oxalate in to zinc oxide. The intense broad band at 3400cm^{-1} **(Figure 2 a–d)** represents the stretching vibration of H-O in crystal water of ZnO. Another broad band at 1650cm^{-1} is superposed by the stretching vibration of C=O and bending vibration of H-O-H. The 3400cm^{-1} and 1650cm^{-1} bands were found to be sharper as the calcination temperature was increased, which indicates the loss of crystal water as the calcination temperature was increased. In the samples calcined at 400^{o}C, a distinct FT-IR band observed at 490cm^{-1} was assigned for Zn-O bonding. From this study it was observed that ZnO synthesized by mechanochemical method and calcined at 400^{o}C shows the formation of Zn-O bond, hence the FT-IR spectra of ZnO synthesized by different methods were also studied for the samples calcined at 400^{o}C.

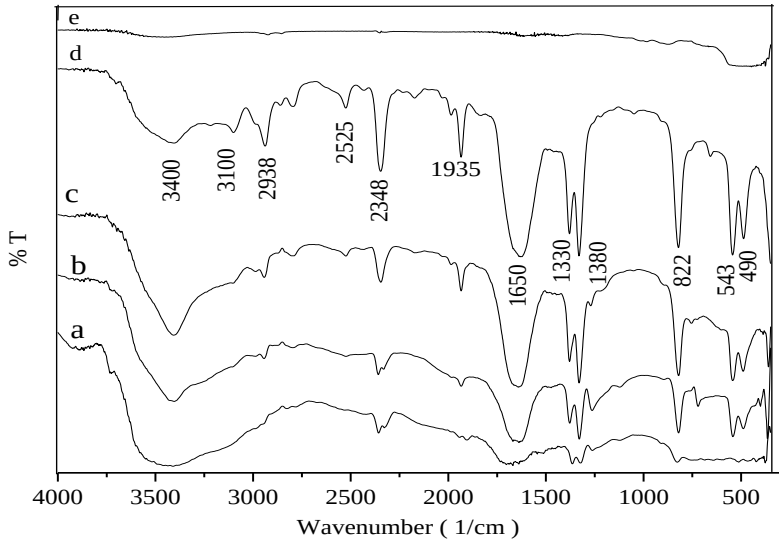

Zinc oxalate before heat treatment (a), Zinc oxalate heated at 100^{o}C (b), 200^{o}C (c), 300^{o}C (d), and 400^{o}C (e)

Figure 2: Changes in FT-IR spectra during the thermal decomposition of zinc oxalate

FT-IR spectra of zinc oxide obtained at 400^{o}C by co-precipitation (P1-Z4, P2-Z4), solid state (S-Z4) and mechanochemical (M-Z4) method displays prominent FT-IR band between 490-500cm^{-1} assigned for Zn-O bonding (**Figure 3)**. FT-IR spectra of these samples also match with that of commercial ZnO. (P1-Z4, P2-Z4), solid state (S-Z4) and mechanochemical (M-Z4) method

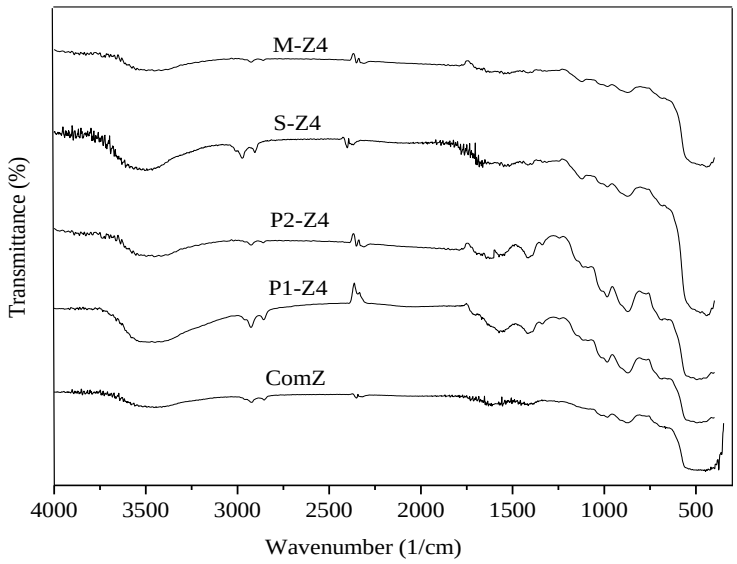

Figure 3: FT-IR spectra of zinc oxide obtained at 400^{o}C, by co-precipitation

3. **XRD analysis: Figure 4** shows XRD pattern of zinc oxide synthesized by different methods. The diffraction peaks of all the samples are indexed to hexagonal wurtzite phase of ZnO (a = 3.249A^{o}, c = 5.206A^{o}) and diffraction data matches to that of JCPDS card No 36-1451, for ZnO. No impurity peaks were observed for any of the synthesized samples. The crystallite size of M-Z4; calculated by Debye-Scherrer formula was found to be smaller than the other samples (**Table 1**). The effect of calcination temperature on crystallite size of ZnO was also studied with XRD pattern. It was found that, as the calcination temperature increases; XRD pattern of ZnO becomes sharper and higher in intensity (**Figure 5**). This is due to increase in crystallite size of ZnO (**Table 1**) which is correlated with photocatalytic activity as discussed in **Section 3.3**.

Table 1: Crystallite size of ZnO

Sample	D (nm)	Sample	D (nm)
M-Z4	34	M-Z5	42
S-Z4	40	M-Z6	54
P1-Z4	59	M-Z7	60
P2-Z4	62	M-Z8	63

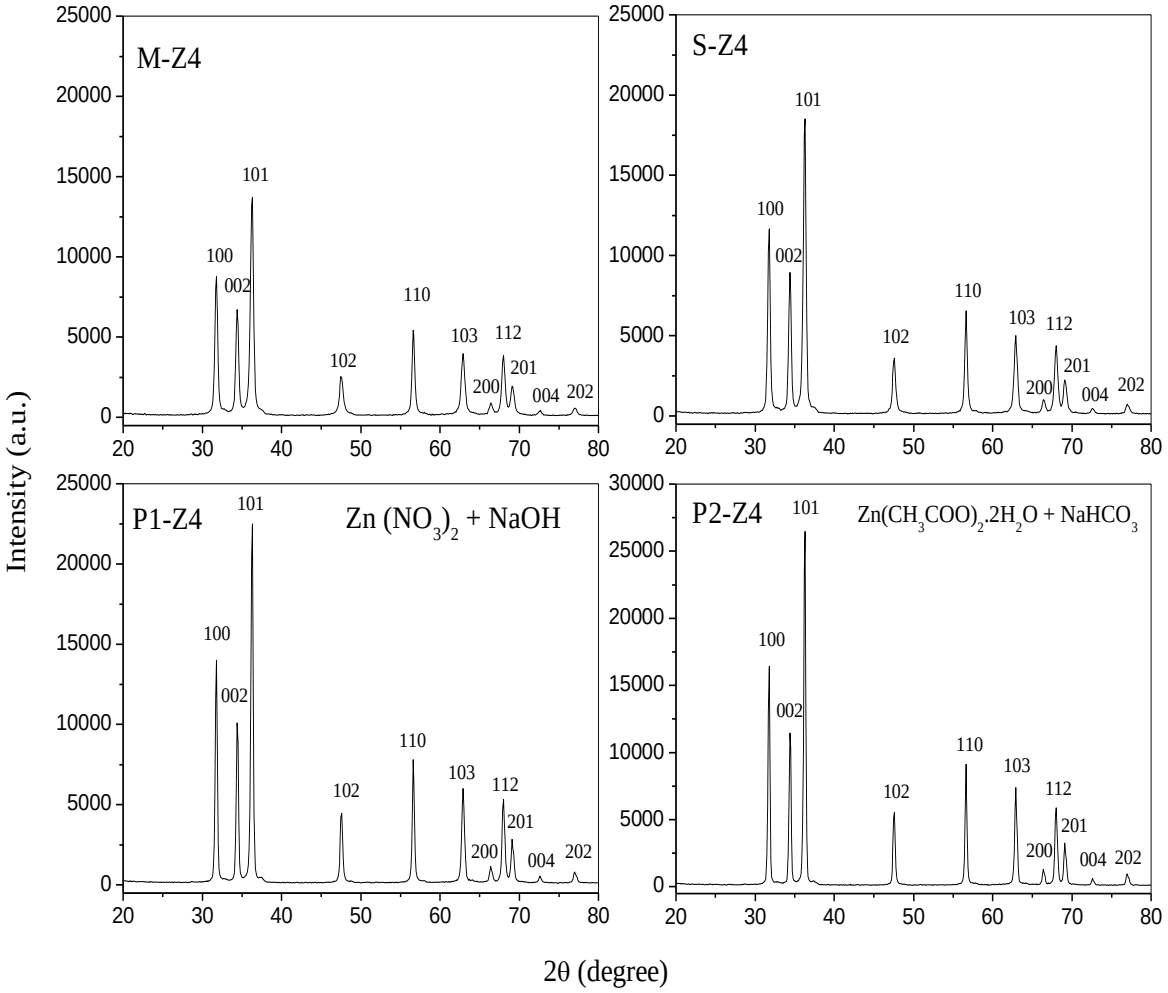

Figure 4: XRD pattern of zinc oxide synthesized by different methods.

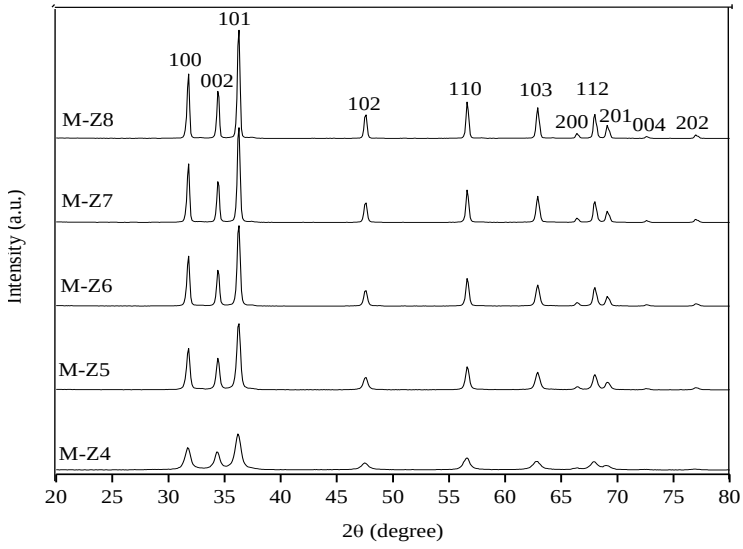

Figure 5: XRD pattern of ZnO synthesized by mechanochemical method and calcined from 400 to 800^{o}C

4. **SEM-EDX analysis:** The zinc oxide synthesized by different methods had rather different morphologies, as shown in **Figure 6.** All the SEM images show that ZnO exists in single homogeneous phase. Zinc oxide synthesized by mechanochemical method (M-Z4) shows tile shaped crystallites while S-Z4 sample displays fibrous nature of crystallites. The zinc oxide synthesized by co-precipitation method (P1-Z4 and P2-Z4) shows agglomerization of crystallites. Thus, SEM analysis supports that, there is no any agglomerization in ZnO synthesized by mechanochemical method. The EDX spectra of M-Z4, S-Z4, P1-Z4 and P2-Z4 show peaks corresponding to Zn and O (**Figure 7**). No any impurity was detected in EDX spectra of these samples. Chemical stoichiometry of ZnO determined by means of EDX results gave an atomic ratio of Zn : O ~ 1 : 1.

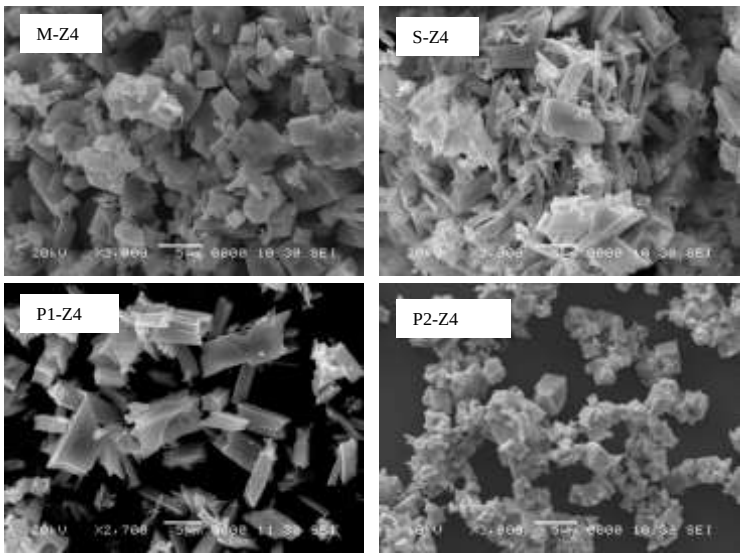

Figure 6: SEM analysis of ZnO synthesized by different methods

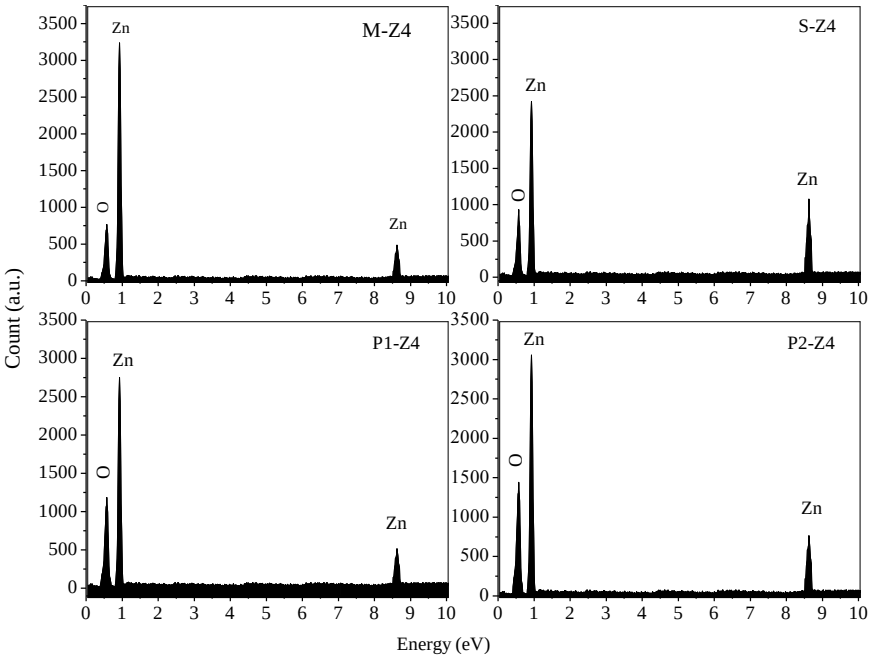

Figure 7: EDX analysis of ZnO synthesized by different methods

Figure 8 displays the SEM images of ZnO synthesized by mechanochemical method and calcined from 500 to 800^{o}C. The morphology of zinc oxide was also greatly affected by calcination temperature.

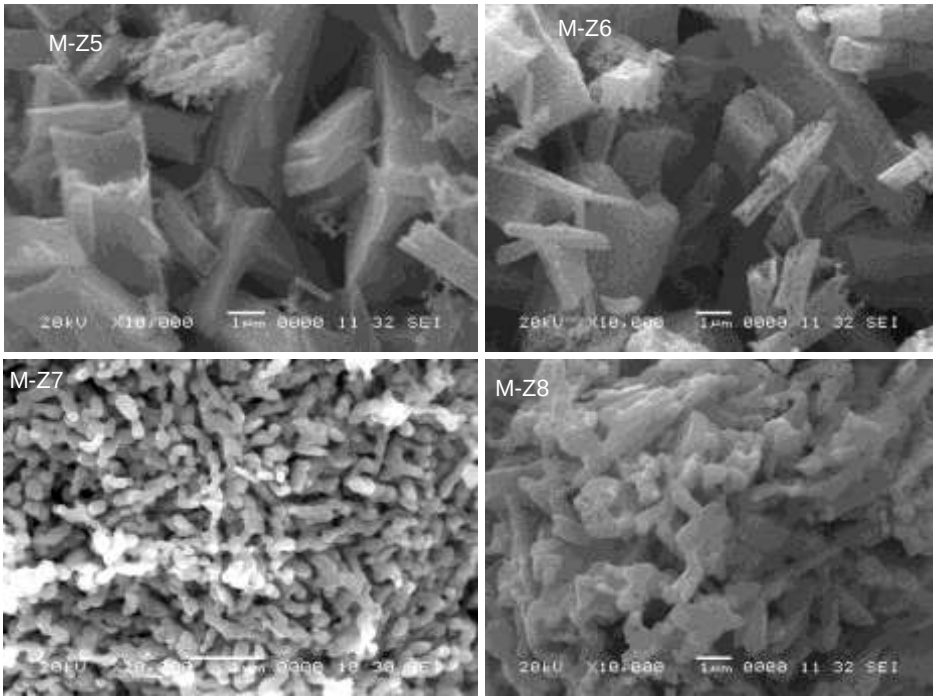

Figure 8: SEM images of ZnO synthesized by mechanochemical method and calcined from 500 to 800^{o}C.

5. **Optical properties of ZnO:** UV-visible absorption and room temperature photoluminescence were used to study the optical properties of the as-synthesized ZnO. The UV-visible absorption spectra of M-Z4, S-Z4, P1-Z4 and P2-Z4 samples dispersed in absolute alcohol are shown in **Figure 9**. All the four samples showed well defined exciton band between 367-373nm, which corresponds to the bulk ZnO absorption **[15].** The absorption in the longer wavelength range (372.5nm) displayed by M-Z4 suggested the existence of more absorption states or defect energy bands in the zinc oxide synthesized by mechanochemical method. Similar observation was reported by Ghoshal et.al. **[16]**. The UV absorption of ZnO synthesized by mechanochemical method was found to shift towards longer wavelength as the calcination temperature increases from 400^{o}C to 800^{o}C (**Figure 10**). This leads to decrease in band gap of ZnO from 3.328 to 3.263 **(Table 2)**. The values of band gap were calculated as per **Equation 2.**

Band gap (eV) $= 1240/\lambda_{max}$ …….. Equation 2

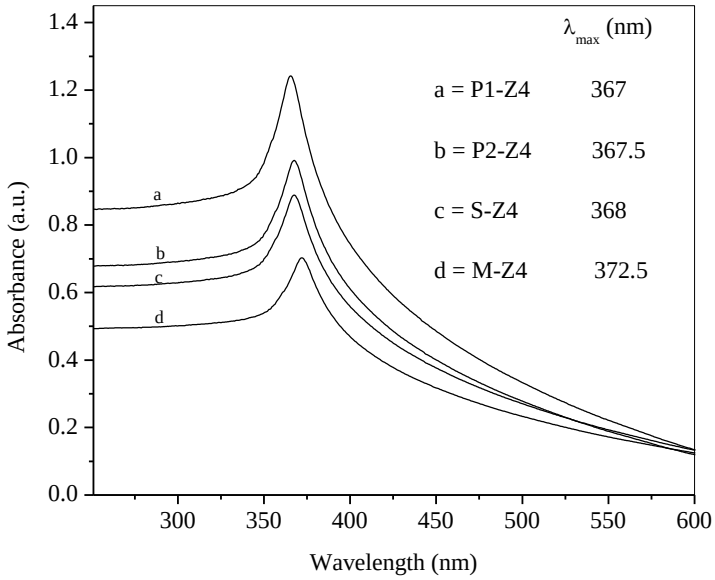

Figure 9: The UV-visible absorption spectra of ZnO synthesized by different methods

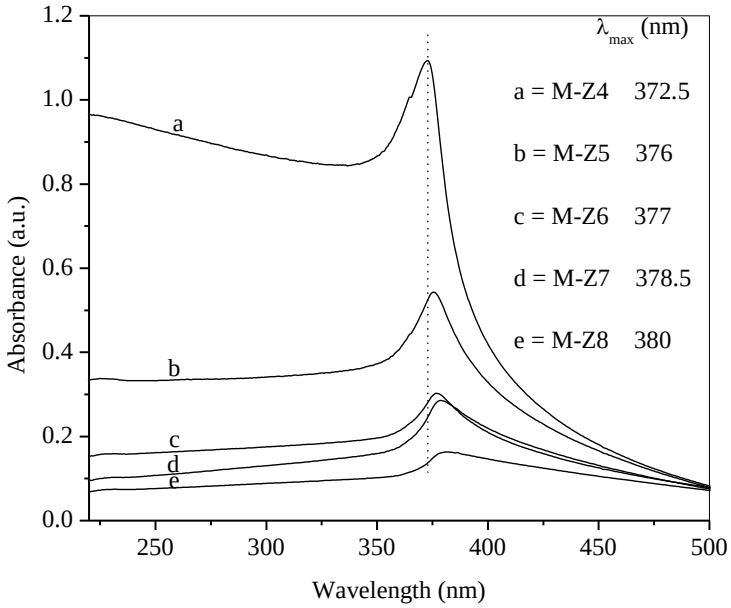

Figure 10: Longer wavelength shift in the UV-visible absorption spectra of ZnO synthesized by mechanochemical method and calcined from 400-800^{o}C

Table 2: Band gap of ZnO synthesized by different methods

Sample	Band gap (eV)	Sample	Band gap (eV)
M-Z4	3.328	M-Z5	3.297
S-Z4	3.369	M-Z6	3.289
P1-Z4	3.378	M-Z7	3.276
P2-Z4	3.374	M-Z8	3.263

The room temperature photoluminescence spectra with an excitation wavelength of 325nm were measured to further characterize the defect features of these ZnO samples. As shown in **Figure 11** all the ZnO samples synthesized by different methods displayed a prominent UV emission peak with maxima at around 390nm; which is ascribed to the excitonic recombination corresponding to the band edge emission of ZnO samples **[17, 18].**

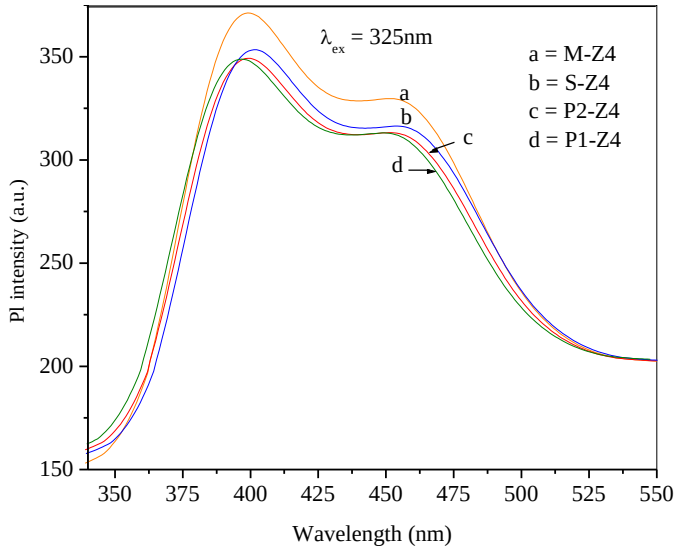

Figure 11: Photoluminescence spectra of ZnO synthesized by different methods

The presence of UV emission at room temperature also confirms the excellent crystallinity of the zinc oxide samples **[19].** In addition to UV emission, all the ZnO samples displays comparatively weak emission band at around 460nm; which is designated as green emission. This green emission originates from the radiative recombination of photogenerated holes with electrons occupying oxygen vacancies **[18]**. **Figure 12** shows the effect of calcination temperature on room temperature photoluminescence of ZnO synthesized by mechanochemical method.

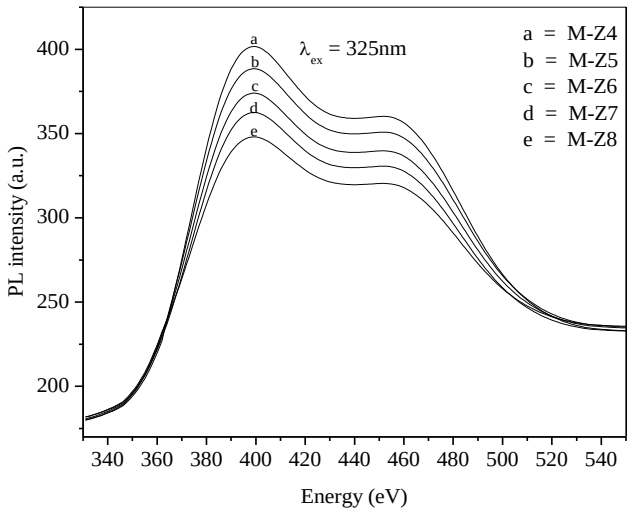

Figure 12: Effect of calcination temperature on room temperature photoluminescence of ZnO synthesized by mechanochemical method

The intensity of green emission was found to decrease with the increase in calcination temperature; this is attributed to decrease in oxygen vacancies and defects. Similar trend in PL intensity was observed for ZnO synthesized by solid state reaction and co-precipitation method and calcined from 400 to 800^{o}C.

6. **XPS analysis:** XPS analysis was used to determine the composition of ZnO. **Figure 13a** shows the whole scanning spectrum of M-Z4. The C1s peak at 284.6 eV was taken as internal standard **(Figure13b).** Fine XPS of Zn_{2p} region is displayed in **Figure 13c.** The peaks located at 1021 eV and 1044 eV are assigned to electronic states of Zn $2p_{3/2}$ and Zn $2p_{1/2}$ respectively, attributed to Zn^{2+} state of zinc. **Figure 13d** shows high resolution XPS of O1s region. In this regard, two contributions may be found: an intense low energy component at 530eV and a high energy component at 531.8eV, both of which can be evaluated using peak fitting. The peak at 529.8 eV was ascribed to O^{2-} ions of ZnO, while another at 531.4 eV is typically related with the lower valence oxygen or adsorbed O_2 **[20].**

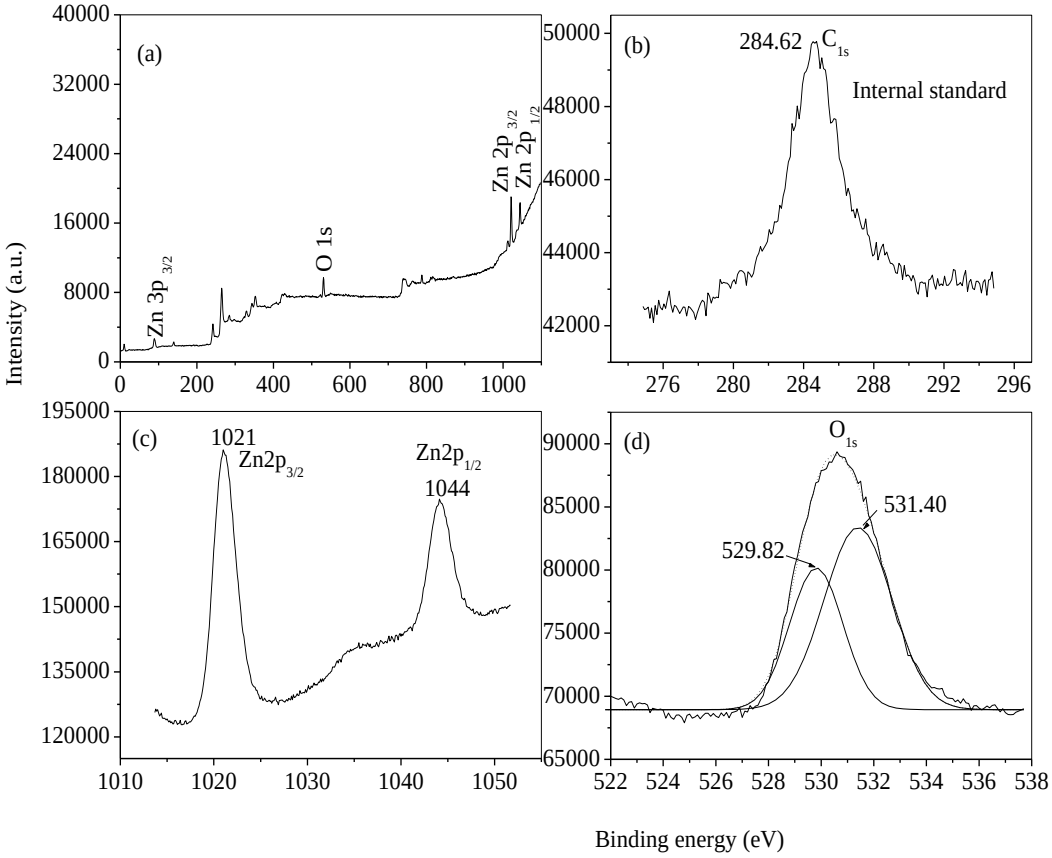

Figure 13: XPS of zinc oxide synthesized by mechanochemical method (M-Z4)

7. **Mechanism of ZnO crystallite growth:** The mechanism of ZnO crystallite growth was investigated as per Scott equation **[21].** The Scott equation is as follows (**Equation 1**).

$$D = C\exp(-E/RT) \quad (1)$$

Where,
D is the XRD average crystal size,
C is a constant (obtained from graph),
E is activation energy for crystallite growth,
R is the gas constant (8.314 × 10-3 kJ mol^{-1} K^{-1}) and
T is absolute temperature (273K).
The plot of ln (D) against 1/T displayed in **Figure 14** depicts straight lines based on the Scott equation, assuming uniform ZnO crystallite growth **[22].**

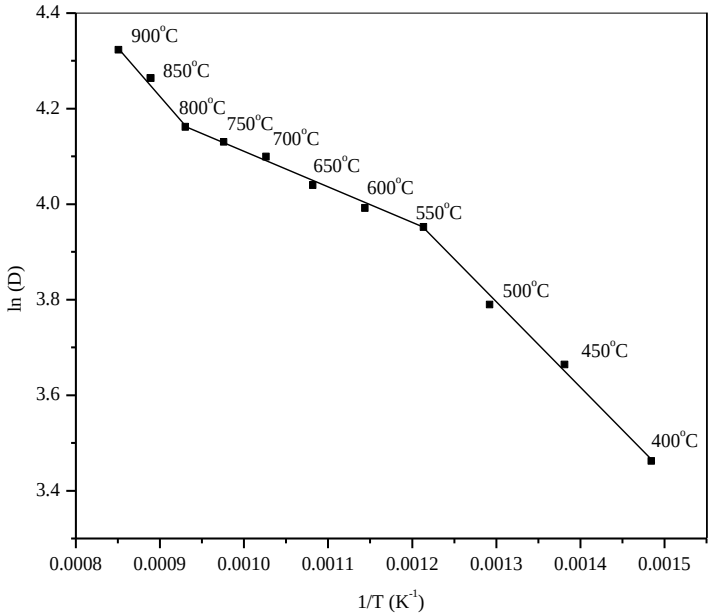

Figure 14: The plot of ln (D) against 1/T

The ZnO calcined at temperatures ranging from 400°C to 900°C has three straight lines with varying slopes. At 550°C, the slope of the first line changes, and at 800°C, the slope of the second line changes. The Scott equation is used to determine the activation energies, 1.88 kJ/mol (E1), 2.48 kJ/mol (E2) and 2.36 kJ/mol (E3) corresponding to crystal formation between 400 and 550 °C, 550 and 800 °C, and 800-900 °C, respectively. This demonstrates that the interfacial response during calcination causes the ZnO crystallite growth rate to vary in different temperature ranges. Because of variations in crystallite form and size, zinc oxide produced at three different crystallite growth rates displayed variable photocatalytic activity. The detail explanation of this is covered in section 3.2.4.

IV. PHOTOCATALYTIC ACTIVITY OF PURE ZINC OXIDE

Photocatalytic activity of zinc oxide synthesized by different techniques in comparison with commercial ZnO was investigated by means of degradation of substrates such as phenol (PHE), resorcinol (RES) and bisphenol A (BPA) in batch photoreactor. Optimization of reaction parameters for maximum degradation of these substrates was done

with ZnO synthesized by mechanochemical method (M-Z4) and results are illustrated in following sections.

1. **Effect of initial concentration of substrate:** The photocatalytic degradation of PHE, RES and BPA at different initial concentrations in the range 50-300 ppm was examined as a result of sunlight irradiation time at the natural pH of suspension (without adjustment) with the loading of 250 mg of M-Z4. 50ppm PHE and BPA as well as 100ppm RES were totally mineralized in to CO_2 and H_2O; which shows zero residual COD (**Table 3**). PCD decreased as the substrate concentration increased over the optimal level (**Figure 15**). This is due to fact that: (a) When the concentration of the substrate surpasses an optimum value, the molecules of the substrate become an impediment to light; hence photons get interrupted before they can reach the ZnO surface, (b) The quantity of adsorption of substrate molecules on the ZnO surface increases with increasing starting concentration; but the number of $^{\cdot}OH$ and $^{\cdot}O_2^-$ radicals produced on the surface of ZnO and the irradiation time are constant.

Table 3: Reduction in residual COD

Conc. (ppm)	PHE		RES		BPA	
	CODi (ppm)	CODt (ppm)	CODi (ppm)	CODt (ppm)	CODi (ppm)	CODt (ppm)
50	123	0	95	0	132	0
100	240	14	190	0	265	58
150	367	54	285	23	397	123
200	482	134	380	76	530	260
250	609	252	475	166	662	404
300	734	461	570	319	795	628

CODi = Initial chemical oxygen demand, CODt = Chemical oxygen demand after 7h irradiation of sunlight. [M-Z4] = 250mg/100ml, pH of suspension = Natural, Sunlight irradiation time = 7h, Intensity of sunlight = 1.7×10^{-7} Einstein S^{-1} cm^{-2}

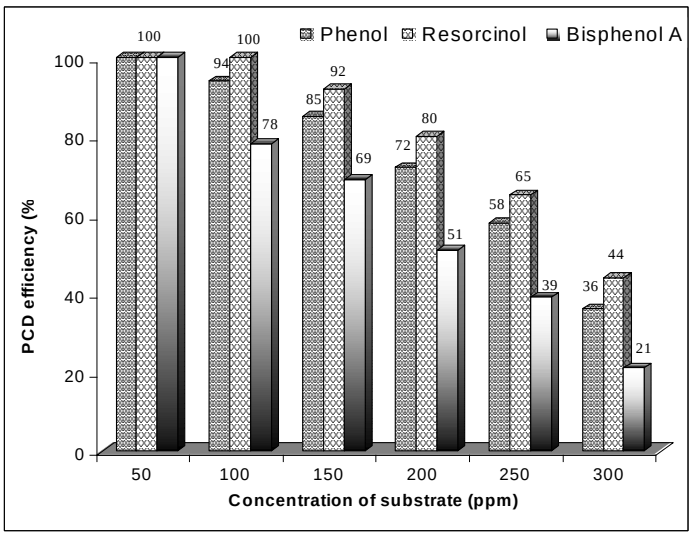

Figure 15: Effect of initial concentration of substrate:

[M-Z4] = 250mg/100ml, pH of suspension = Natural, Sunlight irradiation time = 7h, Intensity of sunlight = 1.7×10^{-7} Einstein S^{-1} cm^{-2}

Therefore, as compared to substrate molecules, the relative number of $^{\cdot}OH$ and $^{\cdot}O_2^-$ radicals available for attacking the substrate decreases. This reduces the PCD of greater substrate concentrations. The optimum substrate concentration for the evaluation of other parameters was determined to be 100 ppm.

2. **Effect of amount of photocatalyst:** To determine the extent to which substrates were 'photolyzed' in the absence of photocatalyst, blank experiments were performed. In the absence of ZnO, no appreciable PCD of substrate was seen in aqueous solution. PCD was detected when an aqueous solution of PHE, RES, and BPA containing ZnO (M-Z4) was exposed to sunshine. This lends credibility of zinc oxide towards solar photocatalytic properties. The optimum quantity of photocatalyst required for maximum PCD of PHE, RES, and BPA was investigated in a slurry approach by adjusting the amount of ZnO in 100ml substrate solution (100 ppm) at its natural pH from 50 to 350mg. The PCD efficiency increased with increasing the amount of ZnO up to 250mg, further increasing the amount of photocatalyst had a unfavorable effect (**Figure 16**).

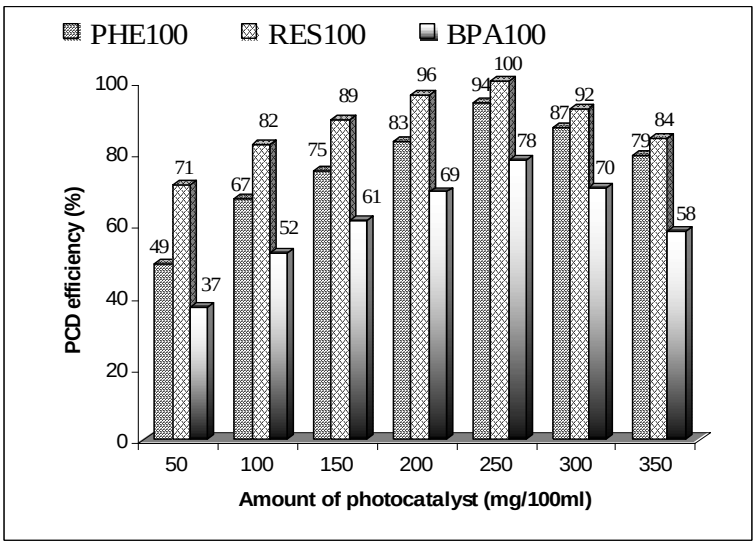

Figure 16: Effect of amount of photocatalyst:

[Substrate] = 100ppm, pH of suspension = Natural, Sunlight irradiation time = 7h, Intensity of sunlight = 1.7×10^{-7} Einstein S^{-1} cm^{-2}

Due to the limited surface area of the photocatalyst, photonic absorption restricts the rate of PCD at lower photocatalyst loading levels than the optimum quantity, hence PCD efficiency improved linearly with increase in photocatalyst loading up to 250mg. Increased photocatalyst amount increases the number of active sites on the photocatalyst surface, resulting in an increase in hydroxyl and superoxide radicals, hence favouring ZnO PCD efficiency. The PCD efficiency declined as the amount of ZnO increased above the limiting point. This is due to an increase in the turbidity of the solution, which decreases sunlight penetration due to increased screening and scattering of light **[23].**

Moreover, after the optimum amount of ZnO, the photocatalyst surface is likely to become unavailable for photoabsorption due to agglomeration and sedimentation of ZnO particles **[24].** In order to monitor the progress of PCD reaction, the chemical oxygen demand of substrate was determined before (CODi) and after the irradiation of reaction mixture with sunlight for 7h (CODt) and results is summarized in **Table 4**.

Table 4: Reduction in residual COD

[M-Z4] mg/100ml	CODt (ppm)		
	PHE100	RES100	BPA100
50	122	55	167
100	79	34	127
150	60	21	103
200	41	08	82
250	**14**	**0**	**58**
300	31	15	79
350	50	30	111

[Substrate] = 100ppm, pH of suspension = Natural, CODi of PHE100 = 240ppm, CODi of RES100 = 190ppm, CODi of BPA100 = 265ppm, Sunlight irradiation time = 7h, Intensity of sunlight = 1.7×10^{-7} Einstein S^{-1} cm^{-2}

The optimum amount of photocatalyst loading selected for the study of other parameters is 250 mg of ZnO.

3. **Effect of initial pH of suspension:** Because most semiconductor oxides are amphoteric in nature, the pH of the suspension is a key parameter influencing the PCD reaction occurring on the surface of the semiconductor particle. It has an effect on the surface charge characteristics of photocatalysts **[25].** The influence of suspension pH on PCD efficiency was investigated from 4 to 10 with 100 ppm substrate solution and 250 mg/100 ml ZnO loading. Before being exposed to sunlight, the pH of the suspension was changed, but it was not measured during the reaction. Every other variable was held constant. As summarized in **Table 5**, the final COD (CODt) was found to be substantially decreased in the pH range of 6 to 7 for PHE100, 7 to 9 for RES100 and 7 for BPA100.

Table 5: Reduction in residual COD

pH	CODt (ppm)		
	PHE100	RES100	BPA100
4	33	74	116
5	24	70	101
6	17	48	82
W.A	**14**	**0**	**58**
7	21	0	66
8	67	0	76
9	77	0	87
10	94	13	130

[Substrate] = 100ppm, CODi of PHE100 = 240ppm, CODi of RES100 = 190ppm, CODi of BPA100 = 265ppm, [M-Z4] = 250mg/100ml, Sunlight irradiation time = 7h, Intensity of sunlight = 1.7×10^{-7} Einstein S^{-1} cm^{-2}

Thus PCD of PHE, RES and BPA was found to be effective in weakly acidic, weakly basic and neutral pH respectively **(Figure 17)**. Because most phenol molecules stay undissociated in mildly acidic conditions, the greatest number of phenol molecules are adsorbed on the surface of zinc oxide. As a result, greater PCD was detected. In alkaline solution, the surface of ZnO is negatively charged, and phenolate intermediates may be repelled away from the surface, preventing phenol molecules from adsorbing on the surface of the photocatalyst **[26].** As a result of this PCD of phenol in alkaline medium was found to be less. The extent of PCD of resorcinol was observed to rise with increasing initial pH of suspension, with maximal PCD up to pH 9 (**Figure 17**).

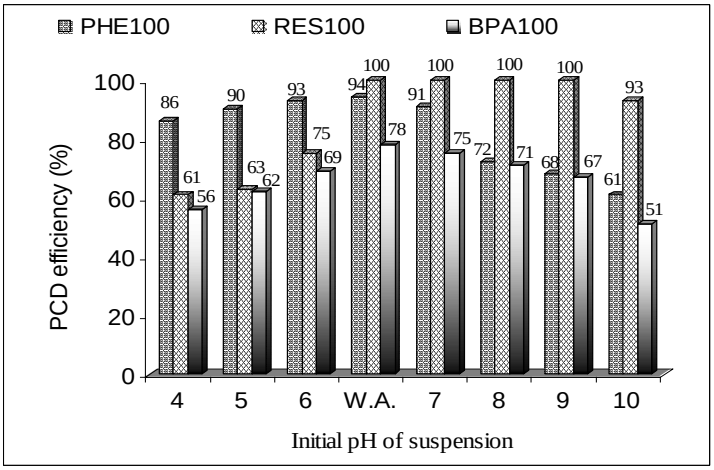

Figure 17: Effect of initial pH of suspension:

[Substrate] = 100ppm, CODi of PHE100 = 240ppm, CODi of RES100 = 190ppm, CODi of BPA100 = 265ppm, [M-Z4] = 250mg/100ml, Natural pH of PHE100 = 5.6, Natural pH of RES100 = 6.8, Natural pH of BPA100 = 6.3, Sunlight irradiation time = 7h, Intensity of sunlight = 1.7×10^{-7} Einstein S^{-1} cm^{-2}, W.A = pH without adjustment (natural).

It is worth noting that no discernible change in resorcinol PCD was seen after pH 9. According to Sakthivel et al **[27],** the acid base property of metal oxide surfaces has a significant impact on their photocatalytic activity. Excess hydroxyl anions in alkaline medium promote photogeneration of •OH radicals, which are recognised as the major oxidising species responsible for PCD. **[28, 29].** This increases PCD of resorcinol in alkaline medium. The pH at zero point charge (zpc) of ZnO is 9.0 ± 0.3. When the suspension pH is greater than pH_{zpc}, the surface of ZnO is negatively charged **[23].** As a result, hydroxyl anions may be repelled away from the negatively charged ZnO surface. Therefore, PCD efficiency was slightly decreased at pH 10. The pH of suspension up to 9 (pH_{zpc} of ZnO) is equally favorable for generation of •OH radicals and adsorption of resorcinol molecules on the surface of ZnO which attributes towards the increase in PCD efficiency. Natural pH of 100ppm phenol, resorcinol and bisphenol A was 5.6, 6.8 and 6.3 respectively. These solutions also showed better photocatalytic degradation therefore other parameters were studied at natural pH of 100ppm substrates.

4. **Effect of calcination temperature:** Photocatalytic efficiency of ZnO is affected by morphology and particle size **[11].** By altering the calcination temperature from 400^{o}C to 800^{o}C, the morphology and crystallite size of ZnO were altered. The PCD efficiency of ZnO calcined from 400^{o}C to 800^{o}C was then examined using solar photocatalytic resorcinol degradation. Zinc oxide calcined from 400^{o}C to 500^{o}C showed 100% PCD efficiency **(Figure 18)** even though particle size of ZnO increases from 34nm to 42nm **(Section 3.2.3, Table 1)**. This may be due to the fact that as crystallite growth rate for ZnO calcined from 400^{o}C to 500^{o}C was uniform (E = 1.88kJ/mol, indicated by Scott equation study), which gives ZnO of same morphology. The PCD effectiveness of ZnO was observed to decline with increasing calcination temperature beyond 500^{o}C. This is because when the calcination temperature rises, the crystallite size of ZnO increases, lowering surface area and hence the number of active photocatalyst sites for substrate adsorption. It is important to note that the crystallite growth rate in temperature range 500^{o}C to 800^{o}C was found to be different (lower) than that of 400^{o}C to 500^{o}C, with higher activation energy (2.48kJ/mol.). Lower crystal growth rate from 500^{o}C to 800^{o}C leads to perfection in crystallization and hence less defective ZnO lattice which is attributed to its poor photocatalytic properties. A similar observation was made by Ao et al **[30]** stating that the variable growth rates of ZnO crystallites in different temperature ranges are owing to distinct interfacial reactions during calcination..

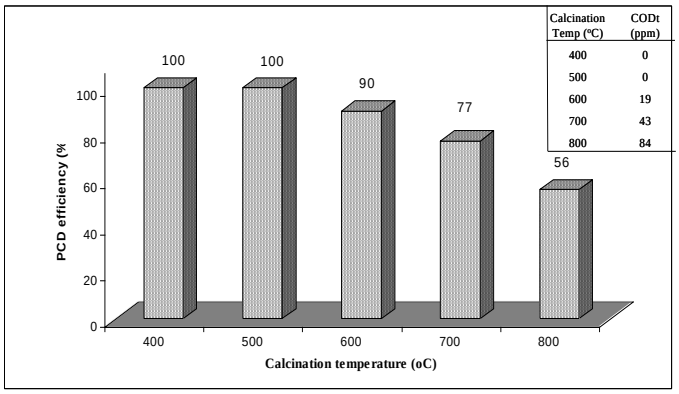

Figure 18: Effect of calcination temperature:

[Resorcinol] = 100ppm, CODi of RES100 = 190ppm, [M-Z4] = 250mg/100ml, Natural pH of RES100 = 6.8, Sunlight irradiation time = 7h, Intensity of sunlight = 1.7×10^{-7} Einstein S^{-1} cm^{-2}

Thus, different morphology of ZnO is affecting its PCD efficiency. When calcination temperature was increased above 800^{o}C, activation energy of zinc oxide crystallite growth was slightly decreased (2.36kJ/mol.) but at the same time particle size were greatly increased which showed negative effect on PCD efficiency (**Figure 18**). Zinc oxide calcined at 400^{o}C (M-Z4) showed 100% photocatalytic degradation of 100ppm resorcinol within 7 hours. This was the lowest possible calcination temperature for the formation of photocatalytically active ZnO. As a result, M-Z4 was chosen to investigate the effect of other parameters such as photocatalyst amount, substrate concentration, pH, and irradiation period.

5. **Effect of irradiation time on PCD efficiency of ZnO:** The influence of irradiation time on zinc oxide PCD efficiency was investigated while maintaining other parameters constant, and the results are shown in **Figure 19**.

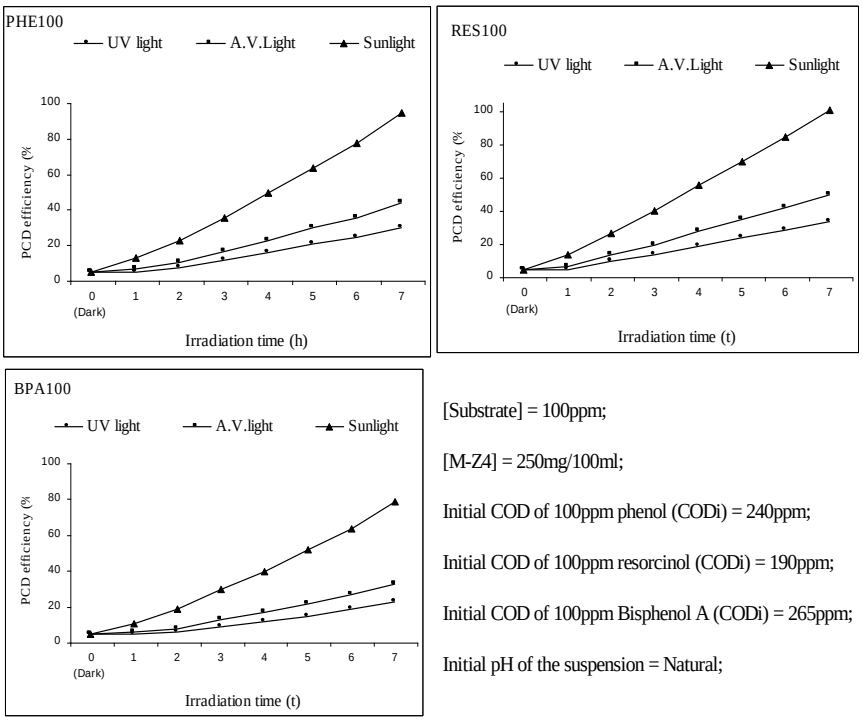

Figure 19: Effect of irradiation time

PCD of substrates were compared under sunlight, U.V. light and artificial visible (A.V.) light from 1000W Xenon lamp. The PCD of substrates over ZnO was found to increase with increase in irradiation time and it was higher in sunlight as compare to UV light or artificial visible light. When 100ppm substrate and ZnO were magnetically agitated for seven hours in the absence of light (dark), little photodegradation was detected; for comparison, zero-hour irradiation was used. (**Table 6**). The residual COD after 1 to 7h irradiation (CODt) of sunlight (SL), Ultra violet light (UV) and artificial visible light (AV) is shown in **Table 6**.

Table 6: Reduction in CODt of phenol, resorcinol and bisphenol A

CODt→	PHE100			RES100			BPA100		
t (h) ↓	UV	AV	SL	UV	AV	SL	UV	AV	SL
0 (Dark)	230	230	230	182	182	182	254	254	254
1	228	225	211	180	178	165	252	250	238
2	223	216	187	172	165	140	251	246	217
3	213	201	156	165	153	115	243	233	188
4	204	187	122	155	138	085	235	223	162
5	192	170	089	146	125	059	227	209	130
6	183	156	055	136	112	030	217	196	098
7	172	138	014	127	097	0	206	180	057

[Substrate] = 100ppm, CODi of PHE100 = 240ppm, CODi of RES100 = 190ppm, CODi of BPA100 = 265ppm, [M-Z4] = 250mg/100ml, Initial pH of suspension = natural. UV = Ultra violet light from 1000W Xenon lamp, AV = Artificial visible light from 1000W Xenon lamp, SL = sunlight.

When 100ppm resorcinol (RES100) containing 250mg/100ml of ZnO (M-Z4) was separately irradiated with SL, AV and UV for 7h; the residual COD was found to be 0, 97 and 127ppm respectively. This shows that zinc oxide is effective photocatalyst in sunlight. Similar trend was observed with PHE100 and BPA100. It is observed that with increase in irradiation time, the absorbance (at λ_{max}) of phenol (270nm), resorcinol (273.8nm) and bisphenol A (276nm) decreases and after 7 hour irradiation of sunlight falls to minimum value (**Figure 20**).

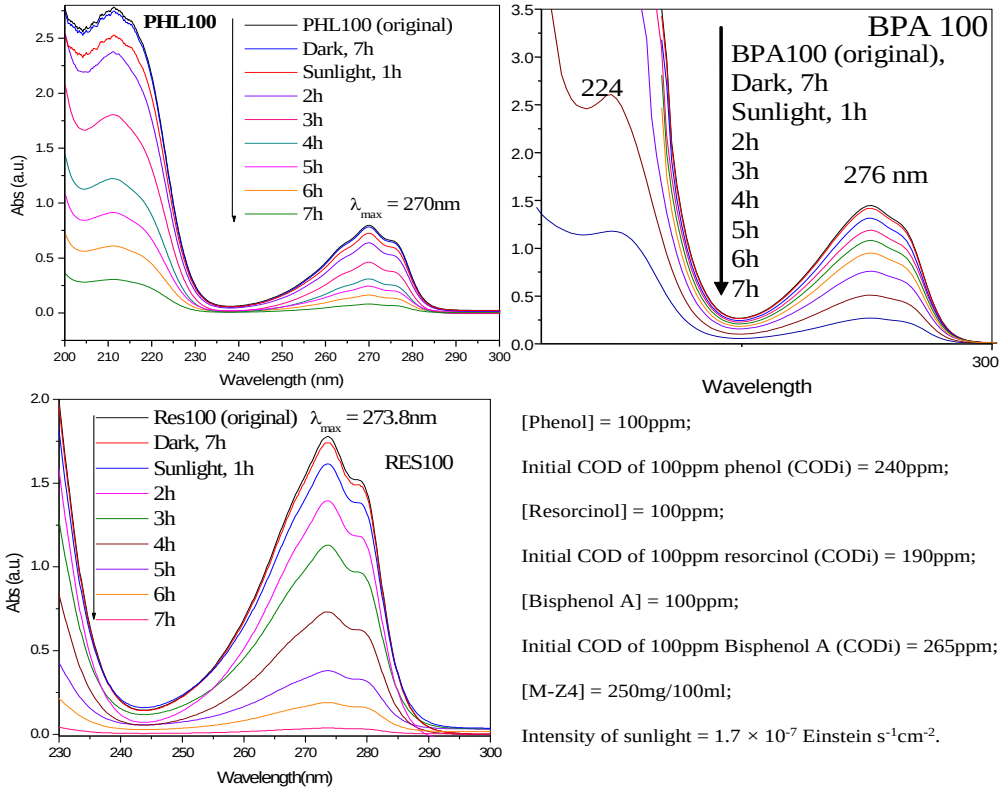

Figure 20: UV-visible spectra showing photocatalytic degradation

6. **Effect of oxidants on PCD efficiency:** The electron-hole recombination stage in the photocatalytic reaction consumes a significant amount of energy and results in a low quantum yield. As a result, preventing electron-hole recombination becomes critical. This can be accomplished by introducing a suitable electron donor (or acceptor) into the system. It has been established that adding an oxidant to a semiconductor suspension increases the rate of photooxidation of organic contaminants. **[31-34].** The commonly used oxidants are $(NH_4)_2S_2O_8$, $KBrO_3$, NaCl and Na_2CO_3. The effect of adding these oxidants on the photocatalytic degradation of 100 ppm phenol has been investigated by varying the amount of oxidant from 50 to 400mg/100ml. From **Figure 21**, it is clear that the addition of $(NH_4)_2S_2O_8$ and $KBrO_3$ increases the PCD of phenol while NaCl and Na_2CO_3 shows negative effect.

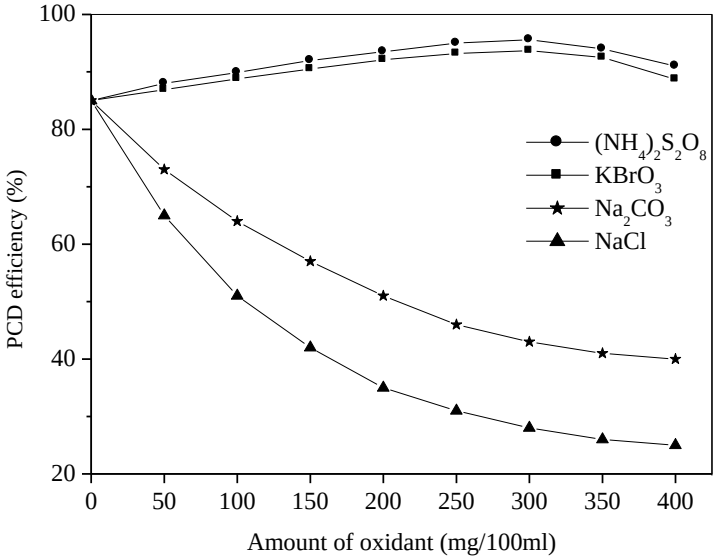

Figure 21: Effect of oxidants on PCD efficiency

[Phenol] = 100ppm, CODi of PHE100 = 240ppm, [M-Z4] = 250mg/100ml, Natural pH of PHE100 = 5.6, Sunlight irradiation time = 7h.

The enhancement of the PCD with $(NH_4)_2S_2O_8$ and $KBrO_3$ is due the suppression of electron-hole recombination and the generation of additional oxidising species **[33]**. The role of $S_2O_8^{2-}$ in the generation of **.**OH by utilizing electrons from conduction band of ZnO is shown in **Scheme 1**.

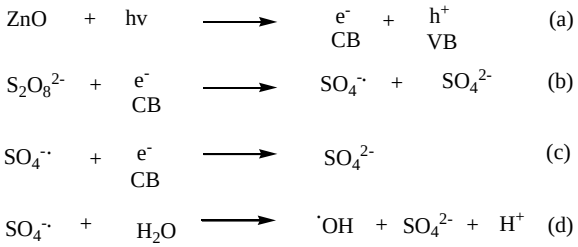

Scheme 1: The role of $S_2O_8^{2-}$ in the generation of ·OH radicals

7. **Comparative study of PCD efficiency of zinc oxide:** Zinc oxide photocatalytic activity synthesised by mechanochemical method (M-Z4), solid state reaction method (S-Z4) and co-precipitation method (P1-Z4, P2-Z4) were compared with that of commercial ZnO and TiO_2, by means of degradation of PHE100, RES100 and BPA100. The optimized parameters such as amount of photocatalyst, concentration of substrate, initial pH of suspension and irradiation time were kept constant. As shown in **Figure 22,** TiO_2 (Degussa P25), was found to be better photocatalyst in UV light, which shows 65% PCD of phenol. Conversely in sunlight, the PCD efficiency of TiO_2 was dropped to 8%. The PCD efficiency of synthesized and commercial ZnO was superior in sunlight than that of UV light. Among the synthesized ZnO samples, M-Z4 displayed highest (94%) PCD of 100ppm phenol in sunlight. The ZnO synthesized by solid state reaction method (S-Z4) shows 84% PCD efficiency. The PCD of phenol over P1-Z4 and P2-Z4 were 75% and 79% respectively, which is higher than that of commercial ZnO (68%). Analogous results

were obtained with RES100 (**Figure 23**) and BPA100 (**Figure 24**). The highest photocatalytic activity of M-Z4 was attributed to more number of oxygen vacancies and defects than other ZnO samples.

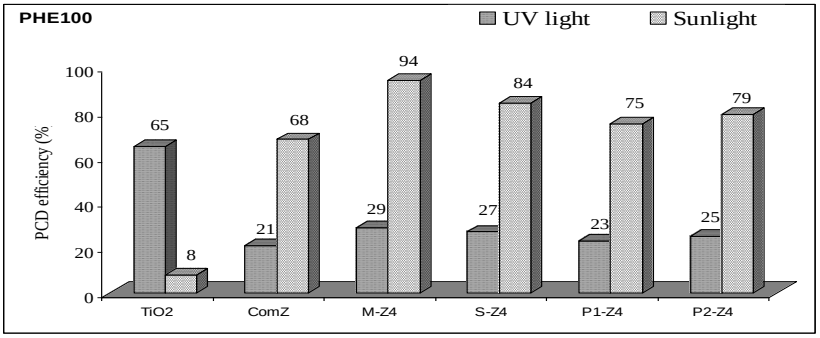

Figure 22: Comparative PCD of phenol over different ZnO samples

[Phenol] = 100ppm, CODi of PHE100 = 240ppm, [photocatalyst] = 250mg/100ml, Natural pH of PHE100 = 5.6, Sunlight irradiation time = 7h.

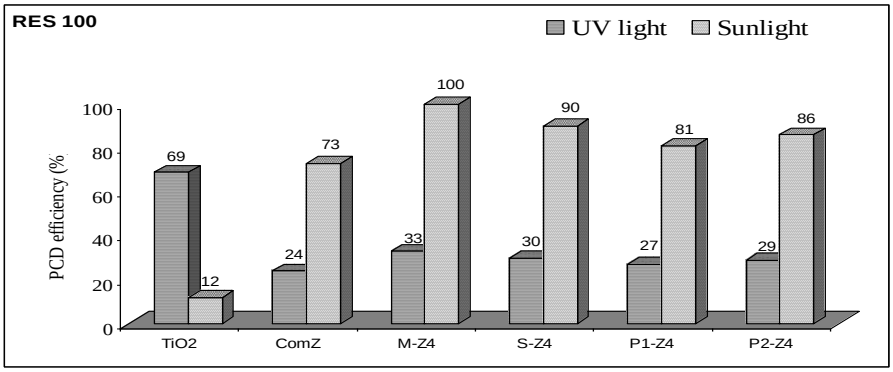

Figure 23: Comparative PCD of resorcinol over different ZnO samples

[Resorcinol] = 100ppm, CODi of RES100 = 190ppm, [Photocatalyst] = 250mg/100ml, Natural pH of RES100 = 6.3, Sunlight irradiation time = 7h.

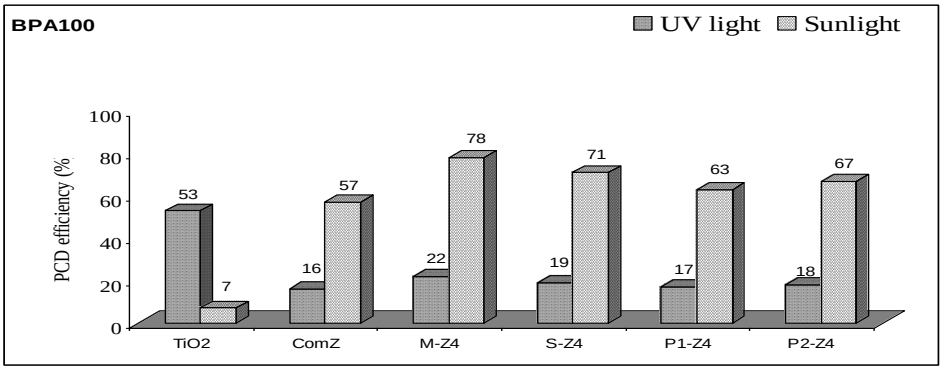

Figure 24: Comparative PCD of bisphenol A over different ZnO samples

[Bisphenol A] = 100ppm, CODi of BPA100 = 265ppm, [Photocatalyst] = 250mg/100ml, Natural pH of BPA100 = 6.3, Sunlight irradiation time = 7h.

V. PHOTOCATALYTIC DEGRADATION MECHANISM

It was discovered that the milky white suspension gradually turned to light brown during the initial time of irradiation. The intensity of brown colour was increased up to 4 hours. After that, as time passed and the irradiation continued, the intensity of the brown colour faded and the milky white suspension reappeared. The brown colour of the photoreaction mixture could be caused by a mixture of reaction intermediates such as benzoquinone, hydroquinone, and catechol. The presence of different intermediates was ensured by HPLC and GC/MS. Solar energy excites the photocatalyst, resulting in the creation of an electron-hole pair **(Scheme 2a)**.

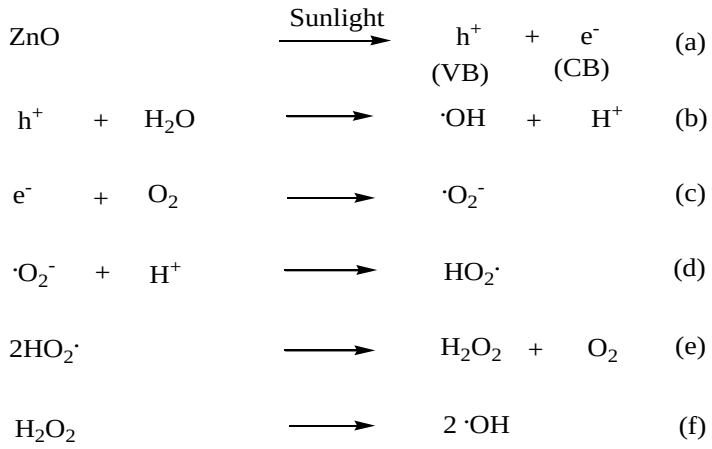

Scheme 2: Formation of an electron-hole pair by excitation of ZnO

The hole combines with water to form ·OH radicals while electron converts the dissolved oxygen to super oxide radical ($\cdot O_2^-$), a strong oxidizing species as shown in **Scheme 2b and c**. The $\cdot O_2^-$ radicals are further converted into $HO_2\cdot$ and ·OH radicals **(Scheme 2d - f).**

1. **Photocatalytic degradation of phenol:** When phenol molecules are adsorbed on the surface of an excited ZnO particle, they are activated via a reaction with the ·OH radical. The hydroxyl radical is electrophilic, preferring to attack the electron-rich ortho or para carbon atoms of phenol. It produces dihydroxycyclohexadienyl (DCHD) radicals, which combine with dissolved oxygen to produce dihydroxybenzenes (DHBs) while also producing $HO\cdot_2$ radical. As illustrated in **Scheme 3**, DCHD radicals are also transformed to phenoxy radicals.

   There are three mesomeric forms of phenoxy radical (**Scheme 4**), which react with ·OH to create benzoquinone, hydroquinone, which are coloured intermediates, and DHBs. The direct reaction of two phenoxy radicals might result in intermediates with two aromatic rings connected by a single bond. **[35].**

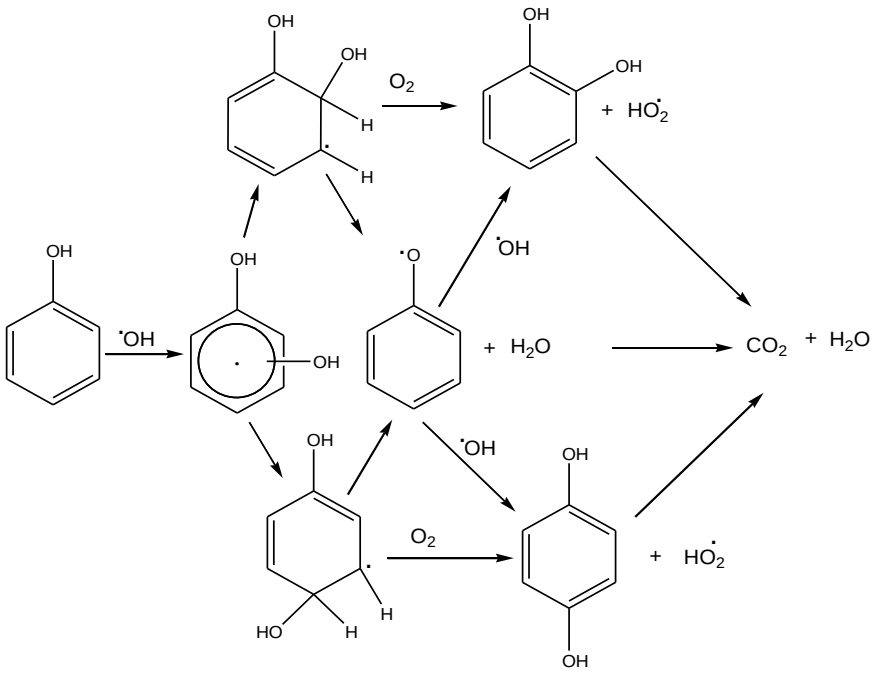

Scheme 3: Photocatalytic degradation of phenol

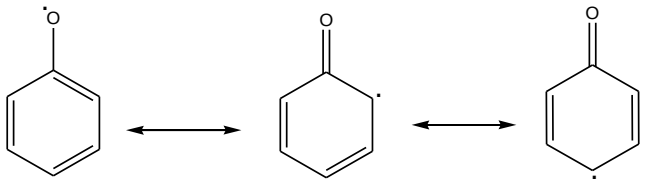

Scheme 4: Mesomeric forms of phenoxy radicals

The use of electron scavenger such as t-butyl alcohol quenches PCD of phenol, suggesting the free radical mechanism for PCD reaction.

2. **Photocatalytic degradation of resorcinol:** When resorcinol molecules bind to the surface of a ZnO particle, they are activated by the .OH radical produced during ZnO photoexcitation. The hydroxyl radical is electrophilic, preferring to attack resorcinol's electron-rich ortho or para carbon atoms. It produces trihydroxycyclohexadienyl (TCHD) radicals, which combine with dissolved oxygen to produce trihydroxybenzenes (THBs), which are coloured intermediates, while also producing $HO._2$ radicals (**Scheme 5**).

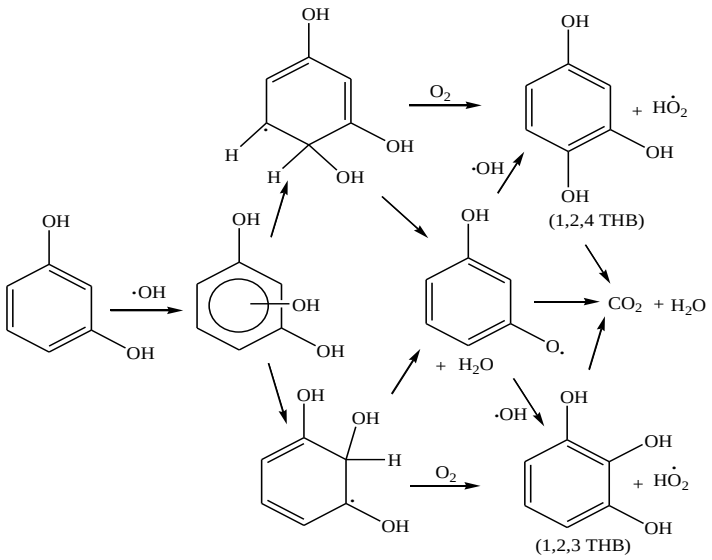

Scheme 5: Photocatalytic degradation of resorcinol

Also, TCHD radicals are transformed to 3-hydroxyl phenoxy radicals, which exists in four mesomeric forms as shown in **Scheme 6**.

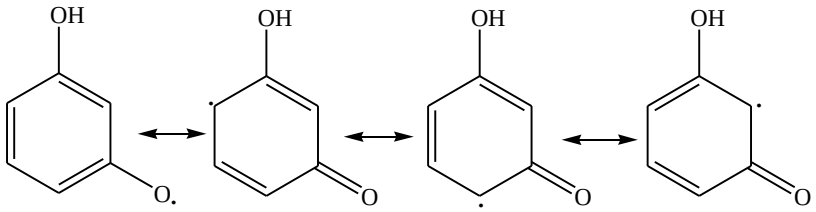

Scheme 6: Mesomeric forms of 3- hydroxyl phenoxy radical

The existence of 1, 2, 3 THB and 1, 2,4THB was confirmed by GC/MS and FT-IR. These 3 - hydroxyl phenoxy radicals can also react with ˙OH to form THBs.

3. **Identification of PCD intermediates of resorcinol: Figure 25** displays the FT-IR spectra of pure resorcinol (a), PCD reaction mixture adsorbed on ZnO after 1h irradiation of sunlight (b), 3h irradiation of sunlight (c), 5h irradiation of sunlight (d), 7h irradiation of sunlight (e), 7h stirring in dark (f) and pure ZnO (g). These spectra show the gradual decomposition of adsorbed resorcinol molecules and PCD intermediates over time. The bands at 1383 cm^{-1} and 1190 – 1155 cm^{-1} (**Figure 25a - d**) are as a result of the interaction between O-H in-plane bending and aromatic C-OH stretching vibrations in resorcinol and intermediates. C=C conjugation and skeletal vibrations of the benzene ring are ascribed to the strong band near 1612 cm^{-1} (**Figure 25a - d**). The strength of the above-mentioned bands decreases with increasing sunlight irradiation time and nearly disappears after 7 hours. (**Figure 25a - e**). In 3hours sunlight irradiation sample (**Figure 25c**), new bands occur at 1726 cm^{-1} and 1287 cm^{-1}, which are most likely caused by 'C=O' stretching vibrations of the generated hydroxyl phenoxy intermediate. (**Scheme 5**). The intensity of the 1383 cm^{-1} and 1190 - 1155 cm^{-1} bands dropped after 3 hours of irradiation (**Figure 25c**), which could be attributed to the conversion of one of the

resorcinol's 'aromatic-OH' groups to the 'C=O' group to produce the hydroxyl phenoxy intermediate. The bands at 1726 cm-1 and 1287 cm-1 are absent in pure resorcinol spectra (**Figure 25a**), but develop in the sample after 3 hours of irradiation (**Figure 25c**) this supports formation of hydroxyl phenoxy radical as a PCD intermediate during irradiation of sunlight (**Scheme 5**). The intensity of 1726 cm^{-1} and 1287 cm^{-1} bands decreases with increase in irradiation time. The distinctive bands of the carbonyl group vanish completely after 7 hours of irradiation (**Figure 25e**). The FT-IR spectra of a 7-hour solar-irradiated sample (**Figure 25e**) and pure ZnO (**Figure 25g**) closely match, indicating that resorcinol is completely degraded after 7 hours of sunlight exposure. An FT-IR spectrum of 7 hour dark adsorption sample (**Figure 25f**) is also almost similar to that of pure ZnO spectra this suggests negligible adsorption and degradation of resorcinol in dark.

The distinctive bands of 'C-H' in plane bending and 'C-H' out of plane bending vibrations of resorcinol's phenyl ring are a weak sharp band at 962 cm^{-1} and a medium band at 848 cm^{-1} in pure resorcinol. The intensity of the 962 - 985 cm^{-1} band declines with irradiation time and disappears after 7 hours of solar exposure (**Figure25b-e**).

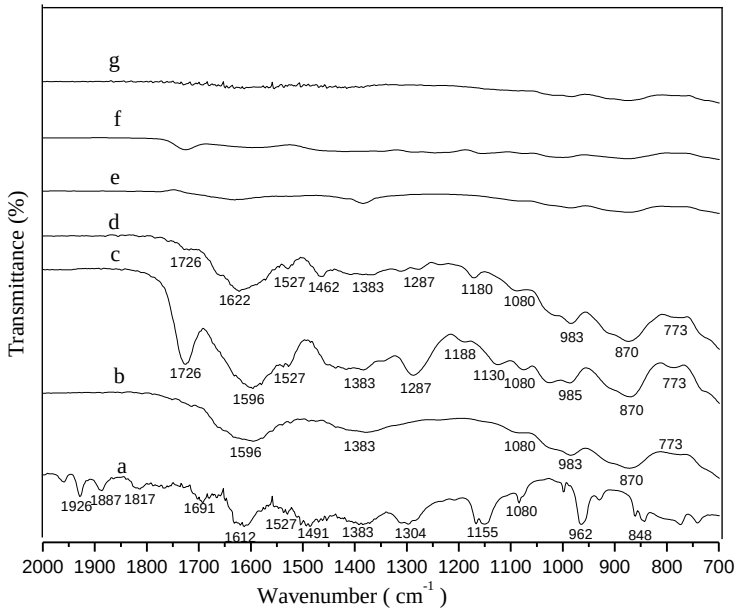

Figure 25: Changes in FT-IR spectra during PCD reaction
FT-IR spectra of: pure resorcinol (a), PCD reaction mixture adsorbed on ZnO after 1h sunlight irradiation (b), 3h sunlight irradiation (c), 5h sunlight irradiation (d), 7h sunlight irradiation (e), 7h stirring in dark (f) and pure ZnO (g).

After 1 hour of solar irradiation, a new, strong band at 870 cm^{-1} develops (**Figure25b-d**), which could be caused by C-H out of plane bending vibrations of two nearby H-atoms of a 1, 2, 4 - trisubstituted benzene ring. This band strongly supports the generation of 1, 2, 4 - trihydroxy benzene intermediates during the PCD process (**scheme 5**). GC-MS validated this as well. Furthermore, the intensity of the 870 cm-1 band grows significantly from 1h to 3h, then diminishes with increasing irradiation time, and finally disappears after 7 hours of sunshine irradiation. (**Figure 25b, c and d**). This suggests that

the generation of intermediates is greatest up to 4 hours after irradiation. A band at 773 cm^{-1} occurs with extremely low intensity in samples taken from 1h to 5h of solar irradiation. (**Figure25b, c and d**) which is the characteristic band of 'C-H' out of plane bending vibrations for 1, 2, 3 – trisubstituted benzene ring of 1, 2, 3 –THB. GC-MS verified the presence of 1, 2, 3 -THB. The intensity of the band at 773 cm^{-1} is relatively low in comparison to the intensity of the band at 870 cm-1, which supports the creation of 1, 2, 4 - THB as a major intermediate and 1, 2, 3 -THB as a minor intermediate (**Scheme 5**). It means para attack of •OH radical dominates over ortho attack. It also supports instability of 1, 2, 3 –THB in comparison to 1, 2, 4 - THB.

4. **Photocatalytic degradation of bisphenol A:** The .OH radicals produced during light excitation have an electrophilic nature and attack the electron rich C4 or C4′ locations in the phenyl groups of BPA [I], resulting in the formation of 4-isopropyl phenol radical [II] and hydroquinone [III] (m/z = 109 + proton) as shown in **Scheme 7**.

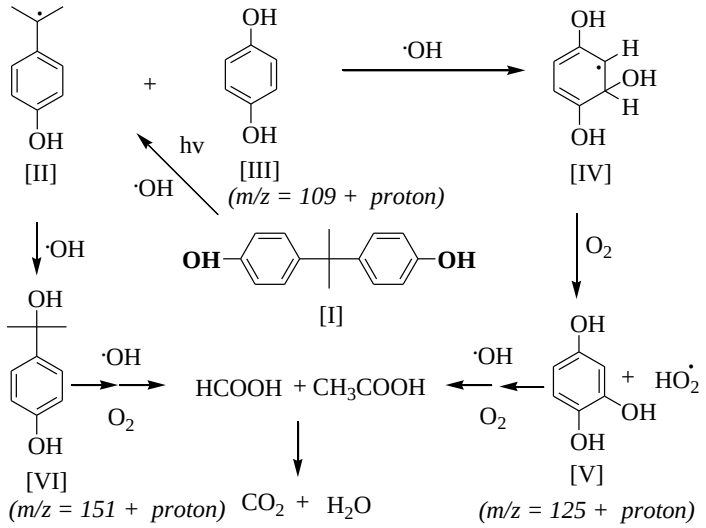

Scheme 7: Photocatalytic degradation of bisphenol A

Hydroquinone is further oxidised by OH radicals to generate the cyclohexa-1, 4-diene-1, 2, 4-triol radical [IV], which is then transformed to benzene-1, 2, 4-triol [V] (m/z = 125 + proton) by reaction with dissolved oxygen. By reacting with .OH radicals, the 4-isopropyl phenol radical is transformed to 4-(2-hydroxypropan-2-yl) phenol [VI] (m/z = 151 + proton). Finally, the species [V] and [VI] oxidise to CO_2 and H_2O. HPLC analysis verified the presence of [III], [V], and [VI] intermediates.

VI. REUSE OF ZINC OXIDE

The photocatalytic activity of recycled ZnO was discovered to be preserved even after the sixth photo degradation experiment. The results are illustrated in **Table 7.** Zinc oxide synthesized by mechanochemical (M-Z4) and solid-state reaction (S-Z4) method retain their PCD efficiency up to 95% and 83% respectively. Zinc oxide synthesized by co-precipitation method (P1-Z4 and P2-Z4) also shows better reusability than that of commercial ZnO.

Table 7: Reuse of ZnO photocatalyst

PCT	Batch I		Batch II		Batch III		Batch IV		Batch V	
	CODt	η (%)	CODt	η (%)	CODt	η (%)	CODt	η (%)	CODt	η (%)
ComZ	52	73	51	73	55	71	57	70	61	68
M-Z4	0	100	0	100	0	100	4	98	10	95
S-Z4	19	90	21	89	20	89	24	87	32	83
P1-Z4	36	81	38	80	42	78	41	78	47	75
P2-Z4	27	86	26	86	30	84	32	83	40	79

[Resorcinol] = 100 ppm; Initial COD = 171 ppm; [PCT] =250mg/100mL; Initial pH = 6.8; sunlight irradiation time = 7h, PCT = Photocatalyst

VII. CONCLUSIONS

TG-DTG and FT-IR study confirms that zinc oxalate synthesized by mechanochemical method is completely converted in to zinc oxide at 400^{o}C. The XRD data of pure ZnO matches to that of JCPDS card No.J.36-1451 indexed for hexagonal wurtzite structure. As calcination temperature of ZnO synthesized by mechanochemical method increases from 400^{o}C to 800^{o}C the crystallite size of ZnO estimated by Scherer's formula was found to increase from 34 to 63nm. The zinc oxide crystallite growth rate studied with Scott equation was found to be different in different calcination temperature range due to the interfacial reaction during calcination**.** Morphology of ZnO was found to be greatly affected by method of synthesis and calcination temperature. The chemical stoichiometry of ZnO was investigated with EDX which gave an atomic ratio Zn : O ~ 1 : 1. UV-Visible spectra show that, ZnO synthesized by mechanochemical method absorbs light of longer wavelength (372.5nm) as compare to other ZnO samples. The strength of UV absorption diminishes when the calcination temperature of ZnO synthesised by mechanochemical technique increases, and the max of zinc oxide changes towards longer wavelength. As a result, the band gap narrows. The PL spectra of ZnO at room temperature show a relatively strong UV emission band corresponding to near band edge (NBE) emission, which is responsible for the recombination of ZnO free excitons, and a weak green yellow emission band originating from deep level (DL) defect emission associated with oxygen vacancies in ZnO lattices. With increase in calcination temperature, PL intensity decreases for ZnO synthesized by mechanochemical method. The XPS peaks located at 1021eV (Zn $2p_{3/2}$) and 1044eV (Zn $2p_{1/2}$) are assigned to Zn^{2+} state and the peak at 529.8eV was attributed to lattice O^{2-} ions of ZnO, while another at 531.4eV is usually associated with the chemisorbed / lower valence oxygen. The crystallite growth rate of ZnO was found to be slowest (E = 2.48kJ/mol) from 550^{o}C to 800^{o}C**.**

The PCD of phenol, resorcinol and bisphenol A (substrates) over ZnO was found to be more effective under solar light in comparison to artificial UV and visible light irradiation. The optimum parameters for maximum PCD efficiency of pure ZnO were determined as 250mg/100mL of ZnO, 100ppm substrate, natural pH of suspension and 7h irradiation of sunlight. It was observed that photodegradation of phenol is favorable in weakly acidic while that of resorcinol and Bisphenol A flattering in neutral as well as weakly basic medium respectively. Lower calcination temperature of photocatalyst (400 to 500^{o}C) favors PCD

efficiency. ZnO synthesized by mechanochemical method shows better PCD efficiency in sunlight. The detailed mechanism of PCD of phenol**,** resorcinol and bisphenol A were proposed with the identification of intermediates such as benzoquinone, hydroquinone, catechol, tri-hydroxy benzenes and 4-(2-hydroxypropan-2-yl) phenol etc. According to FT-IR study, 1, 2, 4-trihydroxy benzene is a major PCD intermediate of resorcinol. Use of oxidants such as $KBrO_3$ and $(NH_4)_2S_2O_8$ with ZnO improves PCD efficiency by 10-20% while that of NaCl and Na_2CO_3 showed negative effect. Zinc oxide can be reused for five times as it undergoes photo corrosion only to the negligible extent.

REFERENCES

[1] K. Honda, A. Fujishima, Nature 238 (1972) 37.
[2] I. Sopyan, M. Watanabe, S. Murasawa, K. Hashimoto, A. Fujishima, J. Photochem. Photobiol. 98 (1996) 79.
[3] B. Dindar, S. Icli, J. Photochem. Photobiol. A: Chem. 140 (2001) 263–268.
[4] M.C. Yeber, J. Roderiguez, J.Freer, J.Baeza, N. Duran,H.D. Mansilla, Chemosphere 39 (1999) 10-16.
[5] M.A. Behnajady, N. Modirshahla, R. Hamzavi, J. Hazard. Mater. B 133 (2006) 226–232.
[6] S. Sakthivel, H. Kish, Chem. Phys. Chem. 4 (2003) 487-490.
[7] A. Mills, S. LeHunte, J. Photochem. Photobiol. 108 (1) (1997) 1–35.
[8] H. Lachheb, E. Puazenat, A. Houas, M. Ksibi, E. Elaloui, C. Guillard, J.M. Herrman, Appl. Catal. B: Environ. 39 (2002) 75.
[9] R.Qiu, D.Zhang, Y. Mo, L. Song, E.Brewer, X.Huang, Y.Xiong, J.Haz.Mat. 156 (2008) 80-85
[10] N.Sobana, M. Swaminathan, Solar Energy Materials and Solar Cells 91 (2007) 727-734.
[11] K.M.Parida, S.Parija, Solar energy 80 (2006) 1048-1054.
[12] D.Li, H.Hadeda, Chemosphere 51 (2003) 129.
[13] F. Lei and B. Yan, J. Phys. Chem. C 113 (2009) 1074-1082.
[14] Z L S Seow, A S W Wong, V Thavasi, R Jose, S Ramakrishna and G W Ho, Nanotechnology 20 (2009) 045604.
[15] A. Pan, R. Yu, S. Xie, Z. Zhang, C. Jin, B. J. Zou, Cryst. Growth 282 (1-2) (2005) 165.
[16] T. Ghoshal, S. Kar, S. J. Chaudhuri, Cryst.Growth 293 (2) (2006) 438.
[17] S.Y. Yu, H.J. Zhang, Z.P. Peng, L.N. Sun, W.D. Shi, Inorg. Chem. 46 (19) (2007) 8019.
[18] M. H. Huang, Y. Wu, H. Feick, N. Tran, E. Weber, P. Yang, Adv. Mater. 13(2) (2001) 113.
[19] L. Xu, Y.L. Hu, C. Pelligra, C.H. Chen, L. Jin, H. Huang, S. Sithambaram, M. Aindow, R. Joesten, S. L. Suib, Chem. Mater. 21 (2009) 2875–2885.
[20] X.H. Wang, S. Liu, P. Chang, Y. Tang, Phys. Lett. A 372 (2008) 2900–2903.
[21] M.G. Scott, Amorphous Metallic Alloys, Butter-Worths Co.Ltd. London, 1983
[22] J. J. Amaral, Mendes, Food and chem. Technol. 40 (2002) 781-788
[23] S. Anandan, A.Vinu, N.Venkatachalam, B. Arabindoo, V. Murugesan, J. Mol. Catal. A: Chem. 256 (2006) 312-320.
[24] C.M.So, M.Y.Cheng, J.C.Yu, P.K.Wong, Chemosphere 46 (2002) 905-912
[25] F.Zhang, J.Zhao, T.Shan, H.Hidaka, E.Pelizzetti, N.Serpone, Appl. Catal. B: Environ.15 (1998) 147-156.
[26] Y. Ku, R.M. Leu, K.C. Lee, Water Research 30 (1996) 2569-2578.
[27] S. Sakthivel, B. Neppolian, M. V. Shankar, B. Arabindoo, M. Palanichamy, V. Murugesan Sol .Energy Mater. Sol. Cells 77 (2003) 65-82.
[28] M. Muruganandham, M. Swaminathan, Sol .Energy Mater. Sol. Cells 81 (2004) 439-457.
[29] A. A. Khodja, T. Sehili, J.F. Pilichowski, P. Boule, J. Photochem. Photobiol. A: Chem. 141 (2001) 231-239.
[30] W. Ao, J. Li, H. Yang, X. Zeng, X. Ma, Powder Technology 168 (2006) 148-151.
[31] N. Daneshvar, D. Salari, A.R. Khataee, J. Photochem. Photobiol. A: Chem. 162 (2004) 317.
[32] S.A. Naman, Z.A.A. Khammas, F.M. Hussein, J. Photochem. Photobiol.A: Chem. 153 (2002) 229.
[33] M. Muneer, D. Bahnemann, Appl. Catal. B: Environ. 36 (2002) 187.
[34] S. Malato, J. Blanco, M.I. Maldonado, P. Fernandez-Ibanez, A. Campos, Appl. Catal. B: Environ. 28 (2000) 163.
[35] A. Peiro, M. Jose, A. Ayllon, J.Perl, X. Domenech, Appl.Catal.B: Environ. 30, (2001) 359-373.

